

# CHANGES OVER TIME IN THE RELATIONSHIP BETWEEN SOLAR ACTIVITY INDICES

© 2025 M.G. Deminov\*, G.F. Deminova

*Pushkov Institute of Terrestrial Magnetism, Ionosphere and Radio Wave Propagation of the Russian Academy of Sciences (IZMIRAN), Moscow, Troitsk, Russia*

\*e-mail: [deminov@izmiran.ru](mailto:deminov@izmiran.ru)

Received January 24, 2025

Revised February 27, 2025

Accepted April 14, 2025

**Abstract.** The results of the analysis of long-term changes in the relationship between solar activity indices for 1957–2022 are presented. For this purpose, the smoothed (using a 24-month filter) indices  $F10$ ,  $F30$ ,  $Ly-\alpha$ ,  $MgII$ ,  $Ri$  and  $IG$  were used: the solar radio emission flux at the wavelengths of 10.7 cm and 30 cm, solar radiation in the Lyman-alpha line of hydrogen (121.567 nm), the ratio of the central part to the flanks in the magnesium emission band of 276–284 nm on the Sun, the international sunspot number and the ionospheric index, which is determined from ionospheric data as an analogue of the sunspot number. It was confirmed that the entire measurement period can be divided into the intervals 1957–1980, 1981–2012 and 2013–2022, in which the relationships between the solar activity indices are clearly different. In the interval 1957–1980, these relationships are stable over time, i.e. there is practically no linear time trend in the dependence of one solar activity index on another. In the 2013–2022 interval, such trends are usually significant. In this interval, the trend  $\Delta IG(X) = IG - IG(X)$  is negative and significant for  $X = F10, F30, MgII, Ly-\alpha$ , or  $Ri$ , where  $IG(X)$  is the average dependence of  $IG$  on  $X$  for this interval.

**Keywords:** *Sun, ionosphere, solar activity index, relationship, long-term change*

**DOI:** 10.31857/S00167940250405e5

## 1. INTRODUCTION

Extreme ultraviolet (EUV) radiation from the Sun is the main source of heating and ionization of the middle and upper atmosphere. Various solar activity indices are used as indicators of the Sun's EUV radiation, including  $F10$ ,  $F30$ ,  $Ly-\alpha$ ,  $MgII$  and  $Ri$  - the Sun's radio emission flux at wavelengths 10.7 cm and 30 cm, solar emission in the Lyman-alpha hydrogen line (121.667 nm), the center-to-flank ratio in the magnesium emission band at 276–284 nm, and the international sunspot number (version 2.0) [Danilov and Berbeneva, 2023; Laštovička and Burešova, 2023; Laštovička,

2024; Mursula et al., 2024]. The correlation between the annual averages of these indices is very high [Laštovička and Burešova, 2023; Mursula et al., 2024]. Nevertheless, the relationship between solar activity indices may be time dependent [Mursula et al., 2024]. It has been noted that the changing relationship between different (e.g., photospheric and chromospheric) solar parameters should be taken into account when using sunspot number or any other single parameter in long-term studies of solar activity [Mursula et al., 2024].

Additional information on the relationships between the solar activity indices can be obtained if the entire measurement period is divided into intervals with different trends of the solar activity index, when the dispersions of the trends for each time interval are much smaller than for the entire measurement period of the analyzed index. The solution of this problem using data of moving annual values of indices  $F10$ ,  $F30$ ,  $Ri$ ,  $MgII$  and ionospheric index  $T$  was given in the first part of this paper [Deminov, 2025].

Moving averages of solar activity indices for a year contain relatively strong fluctuations with characteristic times of less than 1-3 years, making statistical analysis and identification of regularities of solar cycles difficult. Smoothed (using a 24-month Gaussian filter) values of solar activity indices can provide more accurate information on long-term trends of solar activity indices. This filter is used to analyze the patterns of solar cycles, and it is defined by a weight function [Hathaway, 2015]

$$W(t) = \exp(-x^2/2) - (3 - x^2/2) \exp(-2) \quad (1)$$

where  $x = t/12$ ,  $t$  is measured in months, varies from  $t = -23$  to  $t = 23$ , and  $t = 0$  is a given month. From equation (1), it can be seen that  $W(t) = 0$  at  $t = -24$  and  $t = 24$ , so a filter with a weight function  $W(t)$  is called a 24-month Gaussian filter [Hathaway et al., 1999; Hathaway, 2015]. Such a filter almost completely eliminates fluctuations on time scales smaller than 1-3 years and gives one distinct maximum of the solar activity cycle for each of the 24 completed cycles [Hathaway, 2015; Upton and Hathaway, 2023].

The analysis of the properties of such smoothed solar activity indices in the interval 1957-2022, including the relations between the indices and long-term trends of these indices, was the main goal of this work. The results of solving of this problem are presented below: the relationship of the  $Ri$  index with indices  $F10$  and  $F30$ , the relationship of the ionospheric index  $IG$  with all analyzed solar activity indices.

Below, for the sake of brevity, the values  $F10$ ,  $F30$ ,  $MgII$ ,  $Ly-\alpha$ ,  $Ri$  and  $IG$  denote the smoothed (using a 24-month Gaussian filter) values of these indices centered on a given month. In addition, the solar activity indices, which are obtained from the data of measurements of solar

radiation parameters, are named solar indices in contrast to the ionospheric index  $IG$ , which is based on the data of measurements of  $foF2$  - the critical frequency of the ionospheric  $F2$  layer.

## 2. RELATIONS BETWEEN SOLAR INDICES

It was noted above that the correlation between the solar indices is very high; nevertheless, the relationship between them may depend on time. Therefore, it is reasonable to divide the entire measurement period into intervals, in each of which it is necessary to determine the average dependence, for example, of the index  $Y$  on the index  $X$  for the given interval in the form of a stationary regression equation

$$Y(X) = a_{(0)} + a_{(1)}X + a_{(2)}X^2, \quad (2)$$

where the coefficients of this equation are determined from the data set  $Y$  and  $X$  for this time interval. The next step is to identify the linear dependence on time (trend) of the residual of the index  $Y$  from the average for the given interval of the dependence of  $Y$  on  $X$ :

$$\Delta Y(X) = Y - Y(X) = b_0 + b_{(1)}t \quad (3)$$

where  $Y(X)$  is defined by equation (2) with constant coefficients  $a_j$  and the trend of  $\Delta Y(X)$  is determined by the change over time of the indices  $Y$  and  $X$  in equation (3).

This procedure of linear trend extraction  $\Delta Y(X)$  as a correction to  $Y(X)$  dependence taking into account very high correlation between indices  $Y$  and  $X$  has been used repeatedly. It has been used, for example, to extract linear in time trends  $foF2$  (in this case  $Y = foF2$ ,  $X$  is the solar activity index used) [Danilov and Konstantinova, 2023; Laštovička, 2024].

To select the intervals into which the entire measurement period should be divided, we require that these intervals be about 20 years or more, i.e., large enough to reflect the long-term trends of the analyzed indices. In addition, we will require that the variance of the regression equation (3) for each of the selected intervals be much smaller than this variance for the entire measurement period. By analogy with the results presented in the first part of this paper [Deminov, 2025], the entire period of measurements 1957-2022 can be divided into intervals 1957-1980, 1981-2012, and 2013-2022. It can be seen that the last interval is less than 20 years, so the results for this interval can be refined as the data set of solar activity indices expands.

### Table 1

Table 1 shows the parameters of regression equation (3) for  $\Delta Ri(F10)$  and  $\Delta Ri(F30)$ , i.e., the trends of the residual of the  $Ri$  index from the dependencies of  $Ri$  on  $F10$  and  $F30$ . It can be seen from the data in the table that in the interval 1957-1980, the trend of  $\Delta Ri(F10)$  is positive (coefficient  $b_1 > 0$ ), very weak and insignificant, while the trend of  $\Delta Ri(F30)$  is negative (coefficient  $b_1 < 0$ ) and

insignificant. In the interval 1981-2012, the trends of  $\Delta Ri(F10)$  and  $\Delta Ri(F30)$  are negative, for  $\Delta Ri(F30)$  it is maximum in absolute value and significant. In the interval 2013-2022, the trend of  $\Delta Ri(F10)$  is negative, the trend of  $\Delta Ri(F30)$  is positive and they are insignificant or weakly significant. For the whole measurement period 1957-2022, the trends of  $\Delta Ri(F10)$  and  $\Delta Ri(F30)$  are negative and significant, for  $\Delta Ri(F30)$  it is maximum in absolute value. The variance,  $\sigma^2$ , of the trend  $\Delta Ri(F30)$  is larger than that for  $\Delta Ri(F10)$ , for the whole measurement period and each of the selected time intervals. The variance of the trends,  $\Delta Ri(F10)$  and  $\Delta Ri(F30)$ , for the entire measurement period is at least twice the corresponding variance for each of the selected intervals.

The character of changes in the trends of  $\Delta Ri(F10)$  for the selected intervals can be seen more clearly from the data in Fig. 1. It can be seen that not only the dispersion, but also the spread of data for  $\Delta Ri(F30)$  is larger than for  $\Delta Ri(F10)$

### Figure 1.

The relatively low dispersion of the regression equation (3) for each of the selected intervals compared to the entire measurement period is largely due to the consideration of the dependence  $Y(X)$  for each of the selected intervals. In this case, these are the dependencies  $Ri(F10)$  and  $Ri(F30)$ . They are shown in Fig. 2. It can be seen that over time there was an increase in the indices F10 and F30 relative to the index  $Ri$ . This increase in F10 was significant for medium and high solar activity and was almost absent for low solar activity. The increase in the F30 index relative to the  $Ri$  index could occur at any level of solar activity. It has been repeatedly noted that the correlation between solar indices is very high [Laštovička and Burešova, 2023; Mursula et al., 2024]. In this case, for the relationship  $Ri(F10)$  in regression equation (2), the certainty coefficient  $R^2 > 0.996$  and  $\sigma^2 < 2$  for any of the selected time intervals. Similarly,  $R^2 > 0.989$  and  $\sigma^2 < 33$  for the dependence  $Ri(F30)$ .

### Figure 2.

Thus, the relationship between the solar activity indices changed with time. For approximate accounting of these changes, the entire measurement period was divided into relatively large intervals, within which this relationship was assumed constant, and the additional dependence of this relationship on time was accounted for using linear trends of the residuals for each of the selected intervals. In turn, the choice of time intervals was determined by the following conditions: they should be longer than 20 years, the variance of the trend for each interval should be much smaller (approximately 2 times) than its variance for the whole period of index measurements. The intervals 1957-1980, 1981-2012, and 2013-2022 for the trends  $\Delta Ri(F10)$  and  $\Delta Ri(F30)$  met the listed criteria. The 2013-2022 interval is too short, so the results of the trend estimates for this interval, including the value of the coefficient  $b_1$  in equation (3), are preliminary.

The standard characteristics of solar activity cycles are sunspot numbers, in this case, they are indices  $Ri$  - international sunspot numbers (version 2) [Hathaway, 2015]. For the interval 1957-2022, they are shown in Figure 1. From the data in Figure 1, it can be seen that solar cycle heights decreased with time for cycles 21-24. The boundaries of the selected intervals (1981 and 2013) are located in the region of the maxima of cycles 21 and 24, i.e., at the beginning and end of the decreasing cycles. Consequently, changes in the character of the relationships between solar indices are caused by the peculiarities of long-term changes in solar activity cycles and can serve as an additional indicator of such changes in cycles. In this case, cycle 25 was the first cycle with increased height after a series of decreasing cycles. The change in the character of relations between the solar activity indices occurred at the maximum of the previous cycle, i.e., earlier than the beginning of cycle 25.

The conclusion that changes in the character of the relationships between the solar indices can serve as an additional indicator of the trends of changes in solar cycles, including the direction of these changes, was obtained in the first part of this paper [Deminov, 2025]. The results presented here confirm this conclusion. Note that it is the decreasing solar activity cycles 21-24 that correspond to the strong negative trend  $\Delta Ri(F30)$  in Fig. 1.

Additional information on the properties of the solar activity indices can be provided by analyzing the relation of the ionospheric  $IG$  index with the solar indices  $F10$ ,  $F30$ ,  $Ri$ ,  $Ly-\alpha$  and  $MgII$ . The results of this analysis are given below.

### 3. RELATIONS OF THE IONOSPHERIC INDEX WITH THE SOLAR INDICES

Analysis of the relationship between the ionospheric index  $IG$  and solar indices  $F10$ ,  $F30$ ,  $Ri$ ,  $Ly-\alpha$  or  $MgII$  is based on regression equations (2) and (3), where  $Y = IG$ ,  $X = F10, F30, MgII, Ly-\alpha, Ri$  or  $MgII$ . Therefore, for example,  $\Delta IG(F10) = IG - IG(F10) = b_0 + b(1)t$  gives a linear time trend of the index residual  $T$  from which the interval-averaged dependence of  $IG$  on  $F10$  is excluded using regression equation (1) as a polynomial  $IG(F10)$ .

Recall that the indices  $R$ ,  $IG$  and  $MgII$  are dimensionless quantities, the indices  $F10$  and  $F30$  are measured in  $10^{-22}W/(m^2Hz)$ , the index  $Ly-\alpha$  - in  $10^{15}photon/(m^2s)$ . The  $IG$  index is constructed from  $foF2$  median data of ionospheric stations at noon [Liu et al., 1983]. The  $Ly-\alpha$  index is derived from measurements of emission in the Lyman-alpha hydrogen line (121.167 nm) on several satellites, which were calibrated against the most reliable of these data. In addition, for periods of no  $Ly-\alpha$  measurements, the  $Ly-\alpha$  index was derived from regression equations reflecting the relationship of  $Ly-\alpha$  to  $F10$ ,  $F30$ , or  $MgII$ . Consequently, the  $Ly-\alpha$  index data for large time

intervals are composite (composite) data. Version 4 of such composite  $Ly-\alpha$  data was used below [Machol et al., 2019]. The  $MgII$  index is also derived from satellite measurements in the band around 276-284 nm as the ratio of the emission intensity at the center of this band (280 nm) to its flanks [Snow et al., 2019]. The  $MgII$  index data are also composite (composite) data. The daily values of this index start from 07/11/1978, so the smoothed (using a 24-month Gaussian filter)  $MgII$  index data are shown below for the 1981-2012 and 2013-2023 intervals only. For the rest of the smoothed indices centered on a given month, data from 01.1957 r are used.

**Table 2.**

Table 2 shows the parameters of regression equation (3) for  $\Delta IG(X)$ , where  $X = F10, F30, Ri, Ly-\alpha$  or  $MgII$ , for the selected intervals 1957-1980, 1981-2012 and 2013-2022 and the whole measurement period 1957-2022. The exception is the  $MgII$  index, for which there are no measurements in the first time interval. The data in Table 2 show that for the 1957-1980 interval, the trends of  $\Delta IG(X)$  are positive ( $b_1 > 0$ ), but they are low in magnitude and insignificant. For the interval 2013-2023, all the  $\Delta IG(X)$  trends are negative and significant, for trend  $\Delta IG(Ly-\alpha)$  they are maximum in absolute value. For the intermediate interval 1981-2012, the  $\Delta IG(X)$  trends are negative except for the  $\Delta IG(Ly-\alpha)$  trend and they are not significant except for the  $\Delta IG(F30)$  trend.

**Figure 3.**

The features of the trends of  $\Delta IG(X)$  in the selected time intervals can be seen more clearly from the data in Fig. 3. 3. It can be seen that the scatter of data with respect to the trends of  $\Delta IG(X)$  is quite large. Nevertheless, for all considered trends of  $\Delta IG(X)$ , common patterns are clearly distinguished: weak positive trends in the interval 1957-1980 and significant negative trends in the interval 2013-2022.

#### 4. DISCUSSION

The results of the analysis of the smoothed (using a 24-month filter) solar activity indices generally confirm the earlier results of the analysis based on moving averages for a year of these activity indices. Nevertheless, the conclusions presented here on the basis of smoothed 24-month solar activity indices are more accurate, e.g., the dispersions of all trends presented here are about two times smaller than for the trends of annual average indices.

The ionospheric  $IG$  index provides indirect information on the average character of foF2 trends, since it is obtained on the basis of the solution of the inverse ionospheric problem: reduction of errors of the  $foF2$  model with known coefficients [Jones and Gallet, 1962; 1965] using data from a number of ionospheric stations [Liu et al., 1983]. Nevertheless, this indirect information does not

contradict the results of the analysis of  $foF2$  trends from data of specific ionospheric stations. For example, the interval 1957-1980 was chosen as a reference interval for the dependence of  $foF2$  on the solar activity indices, when the linear in time trends of  $foF2$  were practically absent [Danilov and Berbeneva, 2023]. The above results for the  $IG(X)$  trends, where  $X$  is the analyzed solar activity indices, confirmed this conclusion: these trends are not significant for the 1957-1980 interval. The data of  $foF2$  trends at midlatitude stations show an increase in the negative trends in the interval 1996-2022 compared to the previous period [Danilov and Konstantinova, 2023]. The negative trends of the ionospheric index  $\Delta IG(X)$  for all analyzed solar activity indices are also amplified in the interval 2013-2022. Nevertheless, the interval 2013-2022 is too short, so the conclusions about the properties of solar activity indices and their trends for this interval are preliminary.

## 5. CONCLUSIONS.

We present the results of the analysis of long-term changes in the relationship between solar activity indices for 1957-2022. For this purpose, the smoothed (using a 24-month filter) indices  $F10$ ,  $F30$ ,  $Ly-\alpha$ ,  $MgII$ ,  $Ri$ , and  $IG$  - solar radio emission flux at wavelengths 10.7 cm and 30 cm, solar emission in the Lyman-alpha hydrogen line (121.567 nm), the center-to-flank ratio in the 276-284 nm magnesium emission band on the Sun, the international sunspot number, and the ionospheric index, which is determined from ionospheric data as an analog of the sunspot number. The following conclusions are obtained.

1. It was confirmed that the entire measurement period can be divided into the intervals 1957-1980, 1981-2012, and 2013-2022, in which the relationships between the solar activity indices clearly differ. In the 1957-1980 interval, these relationships are stable in time, i.e., there is practically no linear trend in the time dependence of one solar activity index on another. In the 2013-2022 interval, such trends are usually significant. In this interval, the trend  $\Delta IG(X) = IG - IG(X)$  is negative and significant for  $X = F10, F30, MgII, Ly-\alpha$  or  $Ri$ , where  $IG(X)$  is the average for this interval dependence of  $IG$  on  $X$ .
2. The boundaries of these intervals (1980 and 2013) approximately correspond to the maxima of the first and last solar cycles in the regime of decreasing activity, when the solar cycle height decreases with time. The negative trend of  $\Delta IG(F30)$  corresponds to this regime.
3. The results of the analysis of the smoothed (using a 24-month filter) solar activity indices generally confirm the previously obtained results of the analysis based on the moving averages for a year of these activity indices. However, the conclusions obtained on the basis of the smoothed 24-month solar activity indices are more accurate, for example, the dispersions for all the trends

obtained on this basis are approximately two times smaller than for the trends of the annual average solar activity indices.

#### ACKNOWLEDGEMENTS

Solar activity indices data were taken from (<http://www.ukssdc.ac.uk/wdcc1> (WDC for Solar-Terrestrial Physics, UK)), (<ftp.seismo.nrcan.gc.ca/spaceweather> (Space Weather Canada)), ([www.sws.bom.gov.au/HF\\_Systems](http://www.sws.bom.gov.au/HF_Systems) (Space Weather Services, Australia)), (<https://lasp.colorado.edu/lisird> (LASP Interactive Solar Irradiance Datacenter, USA))) 02.12.2024.

#### FUNDING

The research was supported by the Program of Fundamental Scientific Research in the Russian Federation on the theme: "Study of Solar Activity and Physical Processes in the Sun-Earth System" (No. 1021100714181-3).

#### CONFLICT OF INTERESTS

The authors declare that there is no conflict of interest.

#### REFERENCES

1. *Deminov M.G.* Relations between the solar activity indices at different time intervals // Geomagnetism and Aeronomy. T. 65. № 2. 2025.
2. *Danilov A.D., Berbeneva N.A.* Statistical analysis of the critical frequency  $foF2$  dependence on various solar activity indices // Adv. Space Res. V. 72. N 6. P. 2351-2361. 2023. <https://doi.org/10.1016/j.asr.2023.05.012>
3. *Danilov A.D., Konstantinova A.V.* Trends in  $foF2$  to 2022 and various solar activity indices // Adv. Space Res. V. 71. N 11. P. 4594-4603. 2023. <https://doi.org/10.1016/j.asr.2023.01.028>
4. *Hathaway D.H., Wilson R.M., Reichmann E.J.* A synthesis of solar cycle prediction techniques // J. Geophys. Geophys. Res. - Space. V. 104. N 10. P. 22375-22388. 1999. <https://doi.org/10.1029/1999JA900313>
5. *Hathaway D.H.* The solar cycle // Living Rev. Sol. Phys. V. 12. ID 4. 2015. <https://doi.org/10.1007/lrsp-2015-4>
6. *Jones W.B., Gallet R.M.* The representation of diurnal and geographic variations of ionospheric data by numerical methods // Telecommun. J. V. 29. N 5. P. 129-149. 1962.

7. Jones W.B., Gallet R.M. The representation of diurnal and geographic variations of ionospheric data by numerical methods. 2 // Telecommun. J. V. 32. N 1. P. 18-28. 1965.
8. Laštovička J., Burešova D. Relationships between  $foF2$  and various solar activity proxies // Space Weather. V. 21. N 4. ID e2022SW003359. 2023. <https://doi.org/10.1029/2022SW003359>
9. Laštovička J. Dependence of long-term trends in  $foF2$  at middle latitudes on different solar activity proxies // Adv. Space Res. V. 73. N 1. P. 685-689. 2024. <https://doi.org/10.1016/j.asr.2023.09.047>
10. Liu R., Smith P., King J. A new solar index which leads to improved  $foF2$  predictions using the CCIR atlas // Telecommun. J. V. 50. N 8. P. 408-414. 1983.
11. Machol J., Snow M., Woodraska D., Woods T., Viereck R., Coddington O. An improved Lyman-alpha composite // Earth and Space Science. V. 6. N 12. P. 2263-2272. 2019. <https://doi.org/10.1029/2019EA000648>
12. Mursula K., Pevtsov A.A., Asikainen T., Tahtinen I., Yeates A.R. Transition to a weaker Sun: Changes in the solar atmosphere during the decay of the Modern Maximum // Astron. Astrophys. V. 685. ID A170. 2024. <https://doi.org/10.1051/0004-6361/202449231>
13. Snow M., Machol J., Viereck R., Woods T., Weber M., Woodraska D., Elliott J. A revised Magnesium II core-to-wing ratio from SORCE SOLSTICE // Earth and Space Science. V. 6. N 11. P. 2106-2114. 2019. <https://doi.org/10.1029/2019EA000652>
14. Upton L.A., Hathaway D.H. Solar cycle precursors and the outlook for cycle 25 // J. Geophys. Res. - Space. V. 128. N 10. ID e2023JA031681. 2023. <https://doi.org/10.1029/2023JA031681>

Table 1. Parameters of the regression equation (3) for  $\Delta Ri(F10)$  or  $\Delta Ri(F30)$ : the coefficient of this equation  $b_1$  in 1/year, the certainty coefficient  $R^2$  and the variance of  $\sigma^2$  for the intervals 1957-1980, 1981-2012, 2013-2022 and the entire measurement period 1957-2022

1957-1980			1981-2012			2013-2022			1957-2022		
$b_1$	$R^2$	$\sigma^2$	$b_1$	$R^2$	$\sigma^2$	$b_1$	$R^2$	$\sigma^2$	$b_1$	$R^2$	$\sigma^2$
$\Delta Ri(F10)$											
0.03	0.003	12	-0.13	0.152	08	-0.52	0.252	07	-0.26	0.498	25
$\Delta Ri(F30)$											
-0.14	0.050	16	-0.46	0.547	15	0.18	0.009	13	-0.56	0.697	49

Table 2. Parameters of the regression equation (3) for  $\Delta IG(X)$ ,  $X = F10, F30, Ri, Ly-\alpha$  or  $MgII$ : the coefficient of this equation  $b_1$  in 1/year, the certainty coefficient  $R^{(2)}$  and the variance  $\sigma^2$  for the intervals 1957-1980, 1981-2012, 2013-2022 and the whole measurement period 1957-2022.

1957-1980			1981-2012			2013-2022			1957-2022		
$b_1$	$R^2$	$\sigma^2$	$b_1$	$R^2$	$\sigma^2$	$b_1$	$R^2$	$\sigma^2$	$b_1$	$R^2$	$\sigma^2$
$(F10)$											
0.18	0.162	08	-0.00	0.000	12	-1.26	0.772	04	-0.15	0.338	17
$(F30)$											
0.07	0.020	13	-0.26	0.404	08	-0.53	0.399	04	-0.38	0.679	25
$(Ri)$											
0.21	0.244	04	0.105	0.09	09	-0.73	0.445	06	0.048	0.005	15
$(Ly-\alpha)$											
0.00	0.000	14	-0.10	0.04	25	-2.47	0.858	09	-0.44	0.588	51
$(MgII)$											
-	-	-	-0.03	0.009	12	-1.07	0.656	05	-0.25	0.317	19

## Figure captions

**Figure 1.** Changes with time in years of  $Ri$  index, values of  $\Delta Ri(X)$  and their linear trend (thin and thick lines) for the intervals 1953-1980, 1981-2012, 2013-2023 and the whole analyzed measurement period 1953-2023, where  $X = F10$  or  $F30$ . Dots are  $Ri$  values at the boundaries of these intervals.

**Figure 2.** Dependence of the  $Ri$  index on  $F10$  or  $F30$  for time intervals in the years 1957-1980 (thick lines), 1981-2012 (thin lines), and 2013-2023 (dashed lines).

**Figure 3.** Changes with time in years of the values of  $\Delta T(X)$  and their linear trends (thin and thick lines) for the intervals 1957-1980, 1981-2012, 2013-2023, where  $X = F10, F30, Ri$ , or  $Ly-\alpha$ .

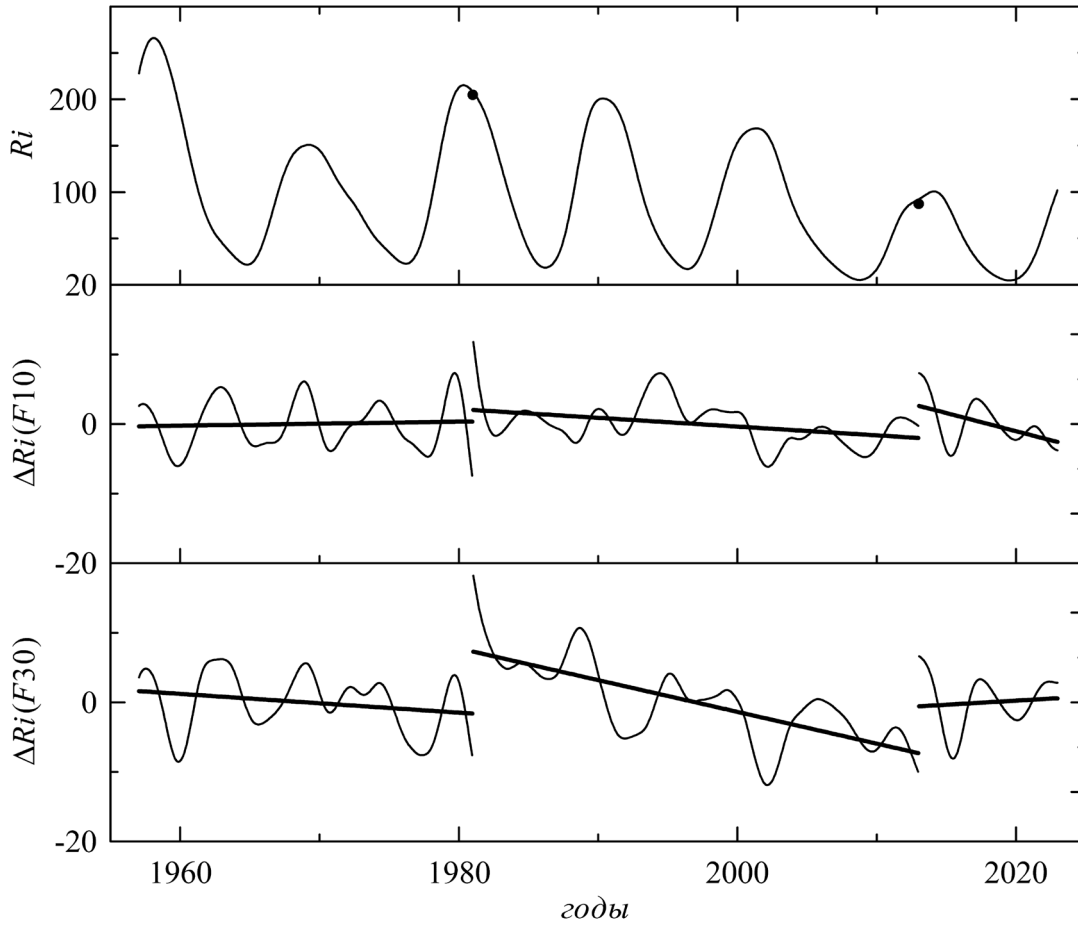


**Figure 1.**

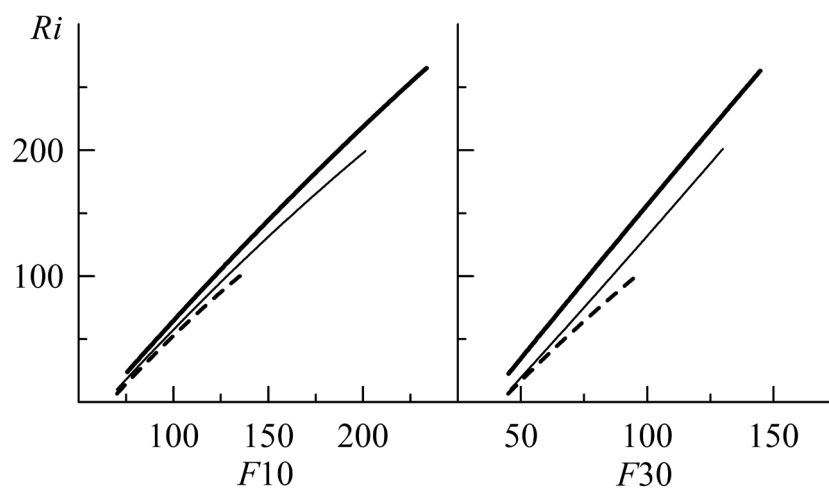


**Figure 2.**

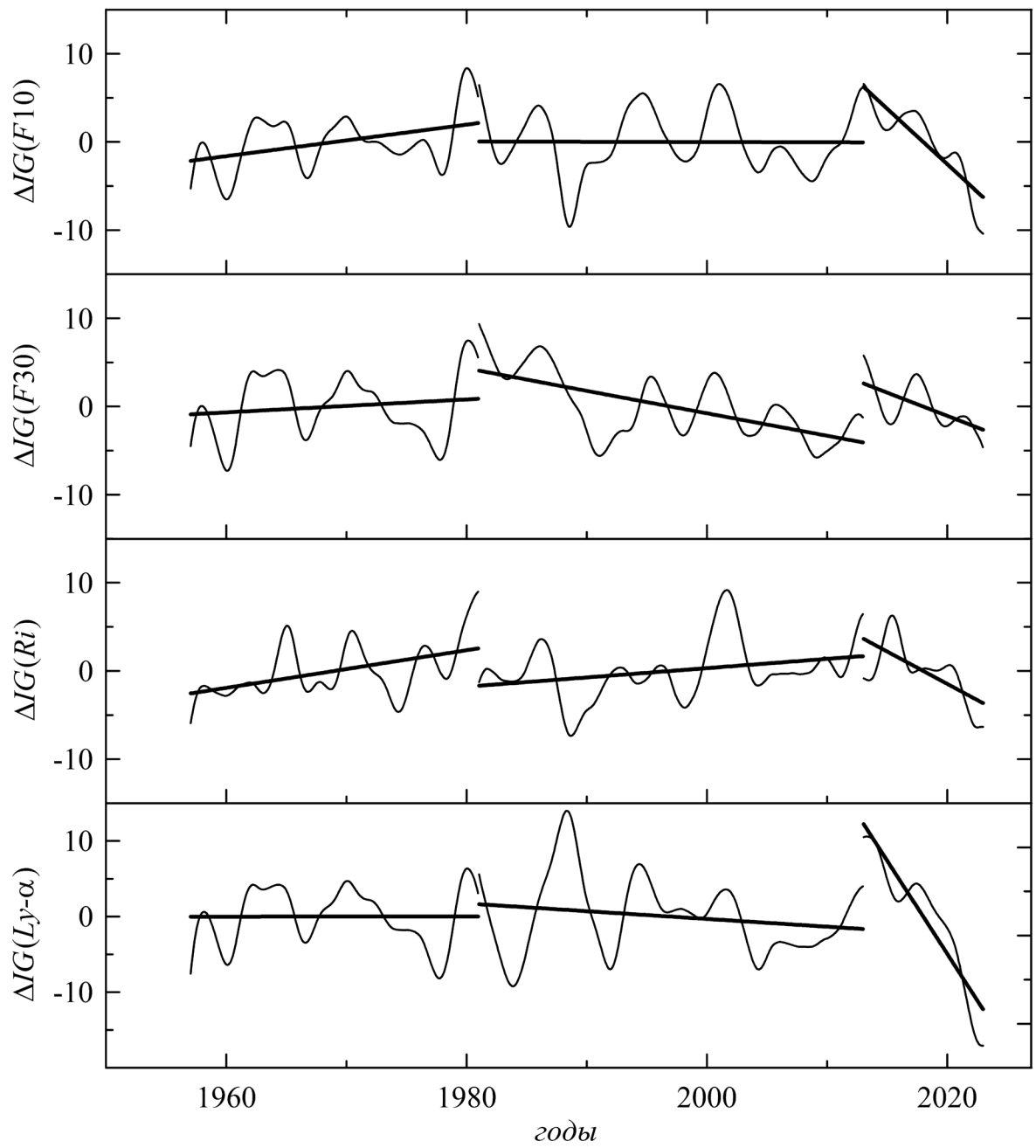


**Figure 3.**